TISSUE ENGINEERING: Part A
Volume 19, Numbers 3 and 4, 2013

DOI: 10.1089/ten.tea.2011.0730



# Fabrication of Blended Polycaprolactone/Poly (Lactic-Co-Glycolic Acid)/β-Tricalcium Phosphate Thin Membrane Using Solid Freeform Fabrication Technology for Guided Bone Regeneration

Jin-Hyung Shim, BS,[1,*] Jung-Bo Huh, DDS, PhD,[2,*] Ju Young Park, MS,[3]
Young-Chan Jeon, DDS, MSD, PhD,[2] Seong Soo Kang, DVM, PhD,[4] Jong Young Kim, PhD,[5]
Jong-Won Rhie, MD, PhD,[6] and Dong-Woo Cho, PhD[1,3]

This study developed a bioabsorbable-guided bone regeneration membrane made of blended polycaprolactone (PCL), poly(lactic-co-glycolic acid) (PLGA), and beta-tricalcium phosphate (β-TCP) using solid freeform fabrication (SFF) technology. The chemical and physical properties of the membrane were evaluated using field emission scanning electron microscopy, energy dispersive spectroscopy, and a tensile test. *In vitro* cell activity assays revealed that the adhesion, proliferation, and osteogenic differentiation of seeded adipose-derived stem cells (ADSCs) were significantly promoted by the PCL/PLGA/β-TCP membranes compared with PCL/PLGA membranes. When the PCL/PLGA and PCL/PLGA/β-TCP membranes were implanted on rabbit calvaria bone defects without ADSCs, microcomputed tomography and histological analyses confirmed that the SFF-based PCL/PLGA/β-TCP membranes greatly increased bone formation without the need for bone substitute materials. Moreover, tight integration, which helps to prevent exposure of the membrane, between both membranes and the soft tissues was clearly observed histologically. The SFF-based PCL/PLGA and PCL/PLGA/β-TCP membranes retained their mechanical stability for up to 8 weeks without significant collapse. Furthermore, PCL/PLGA/β-TCP underwent adequate degradation without a significant immune response at 8 weeks.

## Introduction

Regeneration of mandible and alveolar bone is becoming increasingly important in dental implant and prosthetic dentistry. The guided bone regeneration (GBR) method is widely used for bone regeneration.[1–3] GBR requires a barrier membrane to prevent invasion of soft tissue and to create a space for guiding new bone growth into the bone defect. For clinical success, the GBR membrane must be biocompatible, flexible, and have sufficient mechanical strength. A variety of materials have been used as GBR membranes, such as extended polytetrafluoroethylene[4,5] and titanium,[6,7] which are nondegradable. They have excellent space-making ability with adequate mechanical strength. However, exposure and infection issues are reported frequently.[8,9] This may be attributed to the poor tissue integration ability of nondegradable membranes. Moreover, a second surgical procedure is required to remove the nondegradable membrane after the bone has healed. In comparison, degradable materials such as collagen,[10,11] several synthetic polymers,[12–14] and inorganic ceramics[15,16] do not require a second surgical procedure. Furthermore, using collagen results in superior cell adhesion and proliferation compared to other materials.[17] However, collagen has poor mechanical strength and cannot maintain the space between the membrane and defect site during surgery. Therefore, many researchers have explored thin GBR membranes with various combinations of synthetic biodegradable materials using traditional fabrication methods, such as solvent casting,[18] electrospinning,[13] and a heating press.[16] These methods have some limitations. For example, the solvent casting and electrospinning methods generally require toxic solvents such as chloroform and dichloromethane to dissolve the biodegradable polymers. In addition, it is difficult to create a

[1]Department of Mechanical Engineering, POSTECH, Gyeongbuk, Korea.
[2]Department of Prosthodontics, School of Dentistry, Pusan National University, Gyeongnam, Korea.
[3]Division of Integrative Biosciences and Biotechnology, POSTECH, Gyeongbuk, Korea.
[4]Department of Veterinary Surgery, Chonnam National University, Gwangju, Korea.
[5]Department of Mechanical Engineering, Andong National University, Gyeongbuk, Korea.
[6]Department of Plastic Surgery, College of Medicine, The Catholic University of Korea, Seoul, Korea.
*These two authors contributed equally to this work.

freeform membrane using traditional methods because thickness, pore size, and external shape are not readily adjustable. By contrast, fabricating GBR membranes with a specific shape is simple using solid freeform fabrication (SFF) technology. A complicated two-dimensional or three-dimensional (3D) structure can be fabricated using computer-aided design/computer-aided manufacturing and layer-by-layer processes.[19,20]

In this study, a multi-head deposition system (MHDS; one type of SFF technology) was used to fabricate well-defined GBR membranes using a blend of polycaprolactone (PCL), poly(lactic-co-glycolic acid) (PLGA), and beta-tricalcium phosphate (β-TCP).[21] We have shown that blended PCL/PLGA possesses the biological and mechanical advantages of both PCL and PLGA alone as a 3D scaffold.[22] This study is the first to use blended PCL/PLGA and PCL/PLGA/β-TCP materials as GBR membranes using SFF technology. The characteristics of the fabricated PCL/PLGA and PCL/PLGA/β-TCP membranes were evaluated using field emission scanning electron microscopy (FE-SEM), energy dispersive spectroscopy (EDS), and a tensile mechanical test, which is essential for verifying the utility of the GBR membrane. In addition, *in vitro* experiments examining the cell adhesion, proliferation, and differentiation of the PCL/PLGA and PCL/PLGA/β-TCP membranes were performed using adipose-derived stem cells (ADSCs) for bone regeneration. Recently, ADSCs have been proposed as a promising cell source for bone repair and regeneration. ADSCs proliferate more rapidly than bone marrow-derived stem cells and differentiate into osteogenic lineages.[23] To evaluate the osteogenic capability of the GBR membrane, *in vivo* experiments in rabbit calvarial defects were carried out. We modified the shape of the PCL/PLGA and PCL/PLGA/β-TCP membranes for the *in vivo* experiments. Circular PCL/PLGA and PCL/PLGA/β-TCP membranes (diameter, 10 mm) were prepared on the defect with additional wing parts, including holes for screw fixation. Active new bone formation on the PCL/PLGA and PCL/PLGA/β-TCP membranes was observed at 4 and 8 weeks after implantation using microcomputed tomography (μCT) and histological analysis. No bone substitute material or stem cells were used. Various essential requirements, including tissue integration, space-making ability, and degradability, of the GBR membranes were investigated with the SFF-based PCL/PLGA and PCL/PLGA/β-TCP membranes.

## Materials and Methods

### *Fabrication of SFF-based PCL/PLGA/β-TCP membranes*

**Preparation of blended PCL/PLGA/β-TCP.** PCL (19561-500G, Mw 43,000–50,000; Polysciences), PLGA (430471-5G, Mw 50,000–75,000; Sigma-Aldrich), and β-TCP (average diameter, 100 nm; Berkeley Advanced Biomaterials) were blended using a melting process.[21] Briefly, PCL (0.4 g) and PLGA (0.4 g) granules were melted and mixed in a glass container at 130°C for 10 min. Then, powdered β-TCP (0.2 g) was added to the molten PCL and PLGA, and mixed manually for 5 min. The PCL/PLGA/β-TCP mixture was transferred to a 10-mL steel syringe in the MHDS and maintained at 135°C for dispensing.

**Fabrication of PCL/PLGA/β-TCP membranes using MHDS.** The PCL/PLGA/β-TCP membranes were fabricated using an MHDS, equipped with four heads, in which motion, temperature, and pneumatic pressure are individually controllable.[22] Thus, the MHDS can dispense four different biomaterials into a 3D scaffold or fabricate four scaffolds at the same time. The PCL/PLGA/β-TCP membranes were fabricated layer-by-layer. In total, three layers (each 70 μm high) were stacked to fabricate the membranes. The membranes for the *in vitro* experiments measured $10 \times 10 \times 0.21$ mm. To cover the 8-mm rabbit calvarial defects, circular membranes (diameter, 10 mm) were fabricated, and four wing parts having circular holes (diameter, 1 mm) were constructed every 90° around the circular membrane, to fix the membrane with screws (Appendix Fig. A1).

**SEM/EDS microanalysis of PCL/PLGA/β-TCP membranes.** The morphology of the PCL/PLGA/β-TCP membranes was observed using FE-SEM (SU6600; Hitachi) at 10 kV, and the existence of β-TCP on the surface of the membrane was confirmed using EDS. The membranes were coated with gold using a sputter-coater for 60 s. The surface morphology of the PCL/PLGA/β-TCP membrane was compared with that of PCL/PLGA membranes.

**Mechanical characterization of PCL/PLGA/β-TCP membranes.** The overall size of the membranes used in the mechanical property tests was fixed at $10 \times 10 \times 0.3$ mm. Mechanical testing equipment with a single column (Instron) was used to investigate the tensile property of the membranes at a crosshead velocity of 0.5 mm/min. The tensile property of the PCL/PLGA/β-TCP membrane was compared with that of PCL, PLGA, and PCL/PLGA membranes. The tensile strength was determined using stress-strain curves. The slope of the first linear portion of the stress-strain curve was regarded as the modulus of the membranes. The number of repeats in each group for a statistical analysis in mechanical test was three.[24]

### In vitro *cell activity tests of PCL/PLGA/β-TCP membrane*

**Isolation and culture of human ADSCs.** Human ADSCs were isolated as described previously.[25] Briefly, human subcutaneous lipoaspirates isolated from patients after obtaining informed consent were washed at least three times with phosphate-buffered saline (PBS) (Sigma-Aldrich) to remove contaminating debris and blood. The tissue was digested with 0.05% type I collagenase (Sigma-Aldrich) in PBS for 30 min at 37°C with gentle agitation. After passage through a 25-μm mesh filter and subsequent centrifugation, floating adipocytes were removed from the stromal-vascular fraction (SVF). The isolated human ADSCs in the SVF were cultured in Dulbecco's modified Eagle's medium (DMEM; Gibco BRL) supplemented with 10% (v/v) fetal bovine serum (FBS; Gibco BRL), 100 U/mL penicillin (Gibco BRL), and 0.1 mg/mL streptomycin (Gibco BRL) in humidified air with 5% (v/v) $CO_2$ at 37°C. In addition, osteogenic medium containing 50 μM L-ascorbic acid-2-phosphate (Sigma Aldrich), 10 mM β-glycerophosphate (Sigma Aldrich), and 100 nM dexamethasone (Sigma Aldrich) in complete α-MEM

medium was used to induce the osteogenic differentiation of ADSCs, and the culture medium was changed every 2 days. In this study, human ADSCs were used at the third passage.

Cell seeding and proliferation. The isolated human ADSCs were seeded onto both PCL/PLGA and PCL/PLGA/β-TCP membranes by pipetting 10 μL of a cell suspension containing $1 \times 10^5$ cells.[22] Before seeding the cells, the membranes were prewetted in culture medium for 3 h. The culture medium was refreshed every 2 days. Cell-seeded membranes were incubated for 7 days before counting the number of proliferated ADSCs on each membrane.

Assessment of cell proliferation. A Cell Counting Kit-8 (CCK-8; Dojindo), which is used to measure the number of viable cells in culture medium by detecting dehydrogenates from cells, was used to measure the number of proliferated ADSCs on the membranes (The number of repeats was three). Briefly, the CCK-8 solution was diluted with culture medium (1:10 ratio) and added to each sample. After a 4-h incubation at 37°C, the CCK-8 suspension was extracted. The optical density (OD) of the extracted suspension was measured at 450 nm using a microplate reader (UVM 340; Biochrom). Then, the scaffolds with cells were washed with PBS and incubated continuously with new culture medium.[22]

Reverse transcription–polymerase chain reaction analysis. Total RNA was extracted from the ADSCs, seeded on the PCL/PLGA and PCL/PLGA/β-TCP membranes (The number of repeats was three), using TRIzol reagent (Invitrogen) and was reverse-transcribed with a SuperScript II Reverse Transcriptase (Invitrogen), at day 14 after treatment with osteoblast differentiation medium. The expression of osteoblast marker genes such as alkaline phosphatase (*ALP*) and *Runx2* was analyzed using the real-time quantitative reverse transcription–polymerase chain reaction (RT-PCR). The amplification primers were designed for human *ALP* (5′ primer, ATG TCA TCA TGT TCC TGG GAG AT; 3′ primer, TGG AGC TGA CCC TTG AGG); human *Runx2* (5′ primer, AAC CCA CGA ATG CAC TAT CCA; 3′ primer, CGG ACA TAC CGA GGG ACA TG); and human GAPDH (5′ primer, CCA GGT GGT CTC CTC TGA CTT C; 3′ primer, GTG GTC GTT GAG GGC AAT G). Real-time PCR analysis using SYBR Green was conducted with a LightCycler 2.0 (Roche).

ALP activity. Lysates were isolated from ADSCs seeded onto the PCL/PLGA and PCL/PLGA/β-TCP membranes (the number of repeats was three) at day 14, when the cell seeding density was $5 \times 10^4$ cells/membrane. Lysates from each sample were added to ALP substrate buffer containing 5 mM p-nitrophenyl phosphate (Sigma-Aldrich) and incubated at 37°C for 30 min. The enzymatic activity of ALP was calculated using a *p*-nitrophenol (pNP) standard dilution curve after measuring the absorbance of the pNP product at 405 nm with a microplate reader (UVM 340; Biochrom). The activity was expressed as millimoles of pNP per microgram of lysate protein.

Assessment of calcium deposition. Lysates were isolated from the ADSCs at day 21, and the calcium content of each lysate sample was determined with a QuantiChrom™ Calcium Assay Kit (BioAssay Systems), according to the manufacturer's instructions.[26] To stain calcium deposition of the cells on the PCL/PLGA and PCL/PLGA/β-TCP membranes, the cells were washed three times with PBS and fixed with 5% formaldehyde for 15 min. Then, the cells were stained with Alizarin Red (Sigma-Aldrich) solution (pH 4.3) for 20 min at room temperature and washed with PBS several times to remove nonspecific staining. The area of calcium deposition was observed under a light microscope (Axiovert 200; Zeiss). The amount of calcium deposition was quantified by extracting the Alizarin Red stain from the cells on the membranes using dimethyl sulfoxide (Sigma-Aldrich) at room temperature for 2 h. The extracted Alizarin Red was measured at 570 nm using a microplate reader (UVM 340; Biochrom).[27]

### In vivo *new bone formation analysis*

Animals and operation. Eighteen 12-week-old New Zealand white rabbits (average weight, 3.4 kg; range, 3.3–3.5 kg) were used in this study. This study was approved by the Ethics Committee on Animal Experimentation of Chonnam National University (CNU IACUC-TB-2010-10). For the *in vivo* studies, the animals were divided into control, PCL/PLGA, and PCL/PLGA/β-TCP groups, with 12 animals per group (six at 4 weeks and six at 8 weeks). The animals were premedicated with subcutaneous atropine sulfate (0.05 mg/kg; Huons) and intramuscular xylazine hydrochloride (0.5 mg/kg; Rompun®; Bayer Korea). General anesthesia was induced with intramuscular ketamine HCl (35 mg/kg; Huons). The cranium was shaved from the nasal bone to the occipital protuberance and disinfected with povidone-iodine. Lidocaine (2%) with epinephrine (1:100,000) was infiltrated over the cranium to reduce local hemorrhage. A longitudinal incision was made in the skull, and a midline incision was created in the periosteum. Sharp subperiosteal dissection reflected the pericranium from the outer table of the cranial vault, exposing the parietal bones. A dental-trephine bur was used under copious saline solution to create a bilateral full-thickness calvarial defect. Two 8-mm-diameter defects were created, one on each side of the midline (Fig. 5a). A blended PCL/PLGA or PCL/PLGA/β-TCP membrane was placed on one calvarial defect chosen randomly and fixed with a titanium pin (Dentium) (Fig. 5b). A commercial collagen membrane (CollaTape®; Zimmer Dental) was placed for comparison (Appendix Fig. A2). No statistical analysis was performed because of the insufficient number of collagen membranes. However, no statistical analysis was necessary because all of the implanted collagen membranes collapsed completely, and the soft tissues invaded the defect, obstructing new bone growth. These membranes covered the defect in a manner similar to the GBR technique. The control group was left empty. The pericranium and skin were closed in layers with 3-0 silk sutures. After surgery, the rabbits were given enrofloxacin (Baytril50®, 10 mg/kg; Bayer Korea) and ketoprofen (Ketopro®, 3 mg/kg; Ubtech) intramuscularly once per day for 5 days. Each rabbit was caged individually and received food and water. The observation time points were selected based on a previous study.[8] Nine animals were sacrificed at 4 weeks, and nine were sacrificed at 8 weeks.

Evaluation using μCT. The specimens were wrapped in Parafilm M (Pechiney Plastic Packaging) to prevent drying during scanning. All samples were scanned at 130 kV with an intensity of 60 μA and a resolution of 12 μm pixels, using a bromine filter (0.25 mm; SkyScan-1173 SkyScan®; Kontich). Calibration rods with standardized bone mineral densities were scanned as a reference. Cone-beam reconstruction (ver. 2.15; SkyScan®) was performed. All of the scan and reconstruction parameters were identical for all specimens and calibration rods. The data were analyzed using CT Analyzer (ver. 1.4; SkyScan®). The calibrated 3D images were shown in the gross profiles of the specimens. Since the initial defect was round with an 8.0-mm diameter, the region of interest (ROI) was considered to be the initial size and shape of the defect. The ROI of each specimen was analyzed for bone volume and bone mineral density.

Histomorphometric evaluation. After the radiodensitometry analysis, the calvaria samples were fixed in neutral-buffered formalin (Sigma-Aldrich) for 2 weeks and dehydrated in ascending concentrations of ethanol (70%, 80%, 90%, and 100%). The right and left parietal bones were separated through the midline sagittal suture. The dehydrated specimens were embedded in Technovit 7200 resin (Heraeus KULZER) to show the sagittal sections. A polymerized specimen block was sectioned from the center of each sample using an Exakt diamond cutter (Kulzer Exakt 300; Exakt). The final 15-μm sections were prepared from the initial 400-μm sections by grinding with an Exakt grinding machine (Kulzer Exakt 400CS; Exakt). The specimens were stained with hematoxylin and eosin to evaluate newly regenerated bone and connective tissue. Images were captured using a computer-connected light microscope (Olympus BX) attached to a CCD camera (Polaroid DMC2 digital camera; Polaroid Corp.). The new bone density (%) was measured using SPOT Software V4.0 (Diagnostic Instruments). Only the area with newly formed mineralized bone was measured as new bone area ($mm^2$); marrow, fibrovascular tissue, and fatty tissue were excluded. The new bone density was determined as the percentage of new bone area in the defect area, that is, all tissues within the boundaries of the defect. The specimen images were captured at a magnification of ×12.5, a magnification of ×40 was used for the histometric analysis, and ×100 magnification was used for a precise assessment of new bone area.

### *Statistical analysis*

All data are expressed as means ± standard deviation. Statistical analysis was carried out using Tukey's *post hoc* test of one-way analysis of variance with MINITAB ver. 14.2 software. Values of $p < 0.05$ were taken to indicate statistical significance.

## Results and Discussion

### *Fabrication of GBR membrane using SFF technology*

GBR membranes consisting of PCL/PLGA or PCL/PLGA/β-TCP were successfully fabricated using MHDS. The biomaterials were melted in the MHDS (Fig. 1a) using an installed heater and were dispensed by the MHDS using pneumatic pressure. The fabrication conditions in the MHDS, including pneumatic pressure, temperature, nozzle size, and scan speed, have a significant influence on the flow rate of dispensed materials, which affects line width and height.[28] The pneumatic pressure for the GBR membrane was fixed at 650 kPa, which is the maximum pressure of the MHDS. The fabrication temperatures varied depending on the materials. The viscosity of PCL/PLGA/β-TCP was higher than that of PCL/PLGA at the same temperature, suggesting that β-TCP increases the viscosity of the blended PCL/PLGA/β-TCP. Thus, the flow rate of PCL/PLGA/β-TCP was lower than that of PCL/PLGA at the same temperature and pressure conditions. Based on this observation, the fabrication temperature for PCL/PLGA/β-TCP was increased to 135°C, and that for PCL/PLGA was fixed at

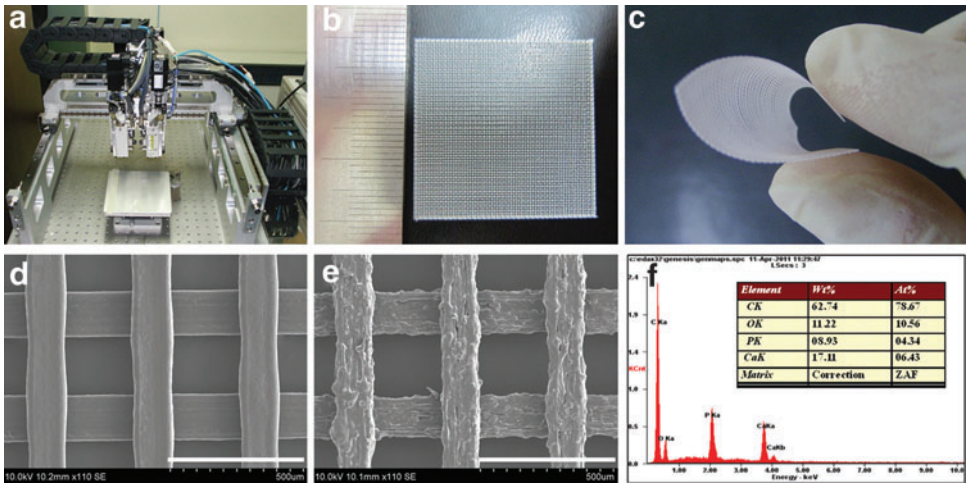


**FIG. 1.** Photographs of **(a)** the MHDS, **(b)** fabricated PCL/PLGA membranes, and **(c)** membrane flexibility. Scanning electron microscopy images of **(d)** a PCL/PLGA membrane (×110, scale bar: 500 μm) and **(e)** a PCL/PLGA/β-TCP membrane (×110, scale bar: 500 μm), and **(f)** energy dispersive spectroscopy analysis of a PCL/PLGA/β-TCP membrane. Well-defined membranes were fabricated using the MHDS. PCL, polycaprolactone; PLGA, poly(lactic-co-glycolic acid); β-TCP, beta-tricalcium phosphate; MHDS, multi-head deposition system. Color images available online at www.liebertpub.com/tea

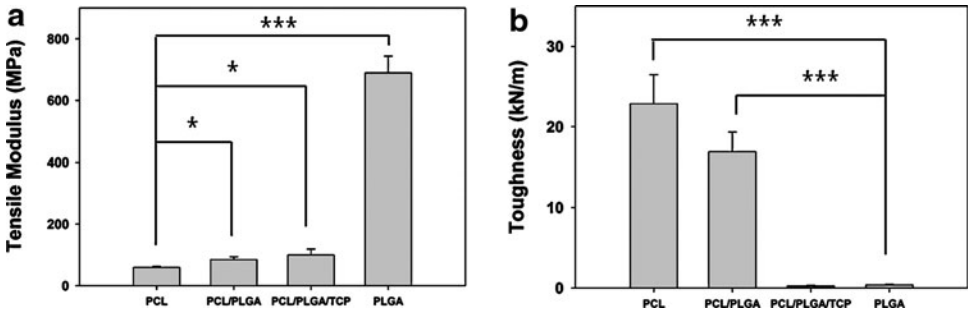


**FIG. 2.** The **(a)** tensile modulus and **(b)** toughness of various membranes. The tensile modulus and toughness were dominantly affected by PLGA and PCL, respectively. The blended PCL/PLGA membrane had a higher tensile modulus and greater toughness than compared with PCL and PLGA, respectively. There were three replicates in each group for the statistical analysis (*$p < 0.05$, ***$p < 0.001$).

125°C. Figure 1b and c show the fabricated mesh-type GBR membrane and the corresponding flexibility. As shown in Figure 1b and d, the fabricated GBR membrane consists of lines and pores, where the line width and pore size were 150 and 250 μm, respectively. Pores in GBR membranes may be involved in the transport of biomolecules for new bone formation and affect the ability of native tissue to penetrate the membrane, allowing the membrane and adjacent tissue to become tightly integrated. Tight tissue integration could eventually eradicate membrane exposure. One distinct advantage of using SFF-based MHDS to fabricate GBR membranes is that the pore size can be controlled. The surface of PCL/PLGA/β-TCP was rougher than that of PCL/PLGA (Fig. 1e). The rough surface of PCL/PLGA/β-TCP, which was attributed to β-TCP, may be advantageous for cell adhesion and tissue integration. EDS analysis confirmed β-TCP on the PCL/PLGA surface and showed that calcium, oxygen, and phosphorous were detectable on the PCL/PLGA/β-TCP membrane surface (Fig. 1f). Moreover, the atomic Ca/P ratio calculated by EDS was 1.48, which is very close to the theoretical Ca/P ratio of 1.5. Thus, β-TCP remained intact during fabrication using the MHDS.

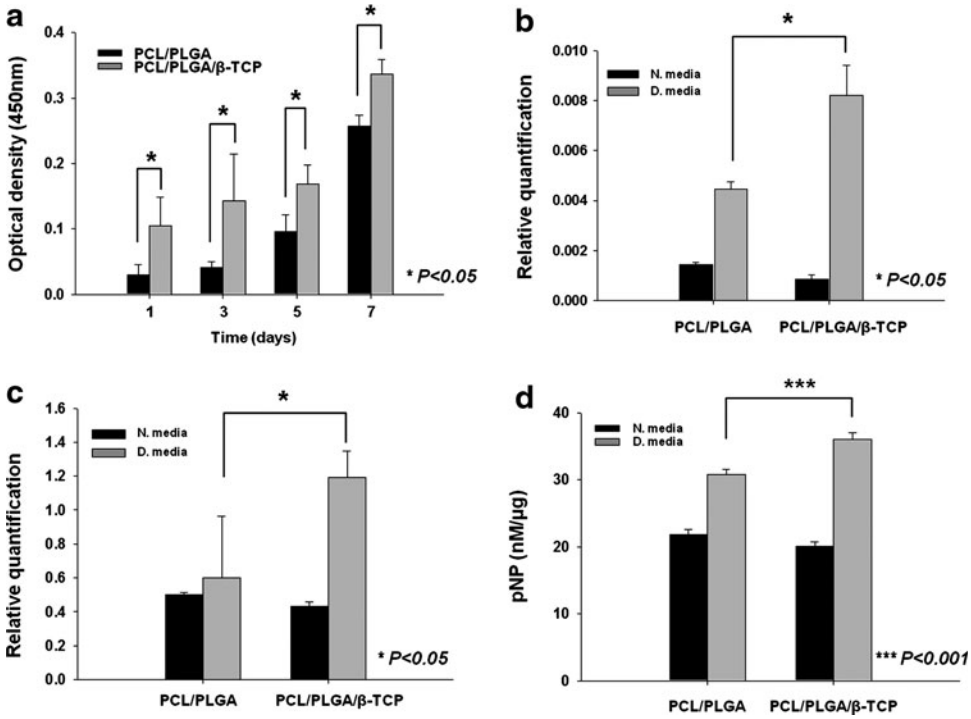


**FIG. 3.** *In vitro* cell activities. **(a)** CCK-8 results for human ADSCs on PCL/PLGA and PCL/PLGA/β-TCP membranes at 1, 3, 5, and 7 days. Expression of **(b)** *ALP* and **(c)** *Runx2* mRNA in ADSCs on PCL/PLGA and PCL/PLGA/β-TCP membranes at day 14. **(d)** ALP activity of ADSCs (normalized to total protein) on PCL/PLGA and PCL/PLGA/β-TCP membranes at day 14. N. medium, normal medium; D. medium, differentiation medium. The ADSCs actively proliferated and differentiated on the membranes, indicating that the PCL/PLGA and PCL/PLGA/β-TCP membranes are cyto-affinitive. In particular, osteogenic differentiation of ADSCs was greater on PCL/PLGA/β-TCP membranes than on PCL/PLGA membranes. There were three replicates in each group for the statistical analysis. ADSC, adipose-derived stem cell; ALP, alkaline phosphatase.

### *Mechanical property of GBR membranes*

The tensile mechanical properties of GBR membranes composed of different biomaterials such as PCL, PLGA, blended PCL/PLGA, and blended PCL/PLGA/β-TCP and fabricated using the MHDS were investigated by analyzing stress-strain curves. The mechanical properties changed significantly depending on the materials used (Fig. 2). PCL membranes tended to elongate without early fracture under a tensile load, which indicates the toughness (total energy a material can absorb before fracture). The toughness of the PCL membrane (22.85 ± 3.64 kN/m) was higher than that of the PLGA, blended PCL/PLGA, and PCL/PLGA/β-TCP membranes (Fig. 2b). However, the degradation rate of PCL is much slower than the regeneration rate of bone.[29] Moreover, the affinity of cells for PCL is inferior to the affinity for PLGA or β-TCP, owing to the high hydrophobicity of PCL.[30,31] In comparison, the tensile modulus of PLGA (689.633 ± 53.94 MPa) was markedly higher than that of the other materials (Fig. 2a). Nevertheless, one major disadvantage of PLGA membranes is that PLGA is very stiff, so that GBR membranes made of only PLGA break easily without elongation under a tensile load. Consequently, the toughness of the PLGA membranes (0.393 ± 0.069 kN/m) was 58 times lower than that of the PCL membranes (Fig. 2b). The stiffness of PLGA precludes its use alone in GBR membranes, even though it has adequate degradation rate and cell affinity. A GBR membrane should be flexible enough to cover irregular bone defects. For PCL/PLGA membranes, the tensile modulus was 1.4 times that of PCL membranes (Fig. 2a), which may be attributable to the blended PLGA, and the toughness was 42 times that of PLGA membranes, possibly due to the blended PCL (Fig. 2b). Thus, the blending of PCL and PLGA allowed each to compensate for the inherent weakness of the other. By contrast, PCL/PLGA/β-TCP was not advantageous in terms of toughness compared with PLGA in the tensile load environment. This was most likely because of the lack of adhesion at the TCP and PCL/PLGA interface. In conclusion, the blended PCL/PLGA and PCL/PLGA/β-TCP possess satisfactory flexibility and space-making ability, and have promising mechanical properties for use in GBR membranes.

### In vitro *cell proliferation result of PCL/PLGA and PCL/PLGA/β-TCP membranes*

The proliferation of ADSCs on PCL/PLGA and PCL/PLGA/β-TCP membranes was evaluated by measuring the OD of the cells. The OD readings of ADSCs at day 1 and over the 7-day culture period were all significantly higher on PCL/PLGA/β-TCP membranes than on PCL/PLGA membranes (Fig. 3a). This may be attributable to the roughness of the PCL/PLGA/β-TCP membrane surface, which can affect cellular activities such as cell morphology, adhesion, and proliferation.[32]

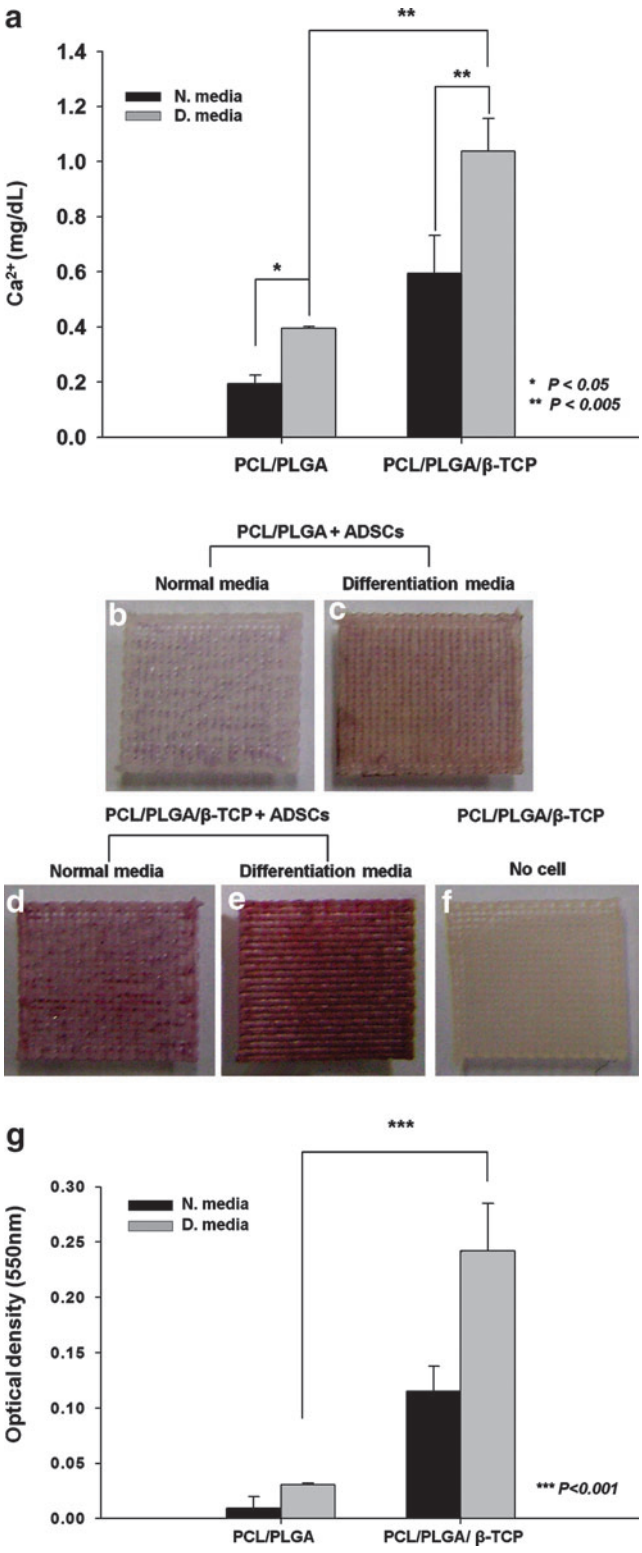


**FIG. 4.** **(a)** The calcium content of ADSCs on PCL/PLGA and PCL/PLGA/β-TCP membranes on day 21, determined using a calcium assay kit. Alizarin Red S staining of **(b, c)** PCL/PLGA and **(d, e)** PCL/PLGA/β-TCP membranes with ADSCs at day 21, and **(f)** PCL/PLGA/β-TCP membranes without ADSCs. **(g)** The quantitative analysis of Alizarin Red S staining. The calcium content and staining intensity of ADSCs were significantly higher on the PCL/PLGA/β-TCP membranes than on the PCL/PLGA membranes. Alizarin Red S did not stain the β-TCP mixed with PCL/PLGA. There were three replicates in each group for the statistical analysis. Color images available online at www.liebertpub.com/tea

### In vitro *cell differentiation results of PCL/PLGA and PCL/PLGA/β-TCP membranes*

To evaluate osteogenic differentiation of ADSCs on the membranes, mRNA expression of the early osteogenic markers *ALP* and *Runx2* was assessed using RT-PCR at day 14. Neither *ALP* nor *Runx2* gene expression in ADSCs cultured in normal medium differed significantly between the PCL/PLGA and PCL/PLGA/β-TCP membranes (Fig. 3b, c). On the other hand, in osteogenic culture medium, the *ALP* and *Runx2* gene expression levels in ADSCs cultured on PCL/PLGA/β-TCP membranes were 1.82 and 2 times, respectively, those on PCL/PLGA membranes (Fig. 3b, c). ALP activity was also examined at day 14 (Fig. 3d). Similarly, in normal culture medium, ALP activity did not differ significantly between the PCL/PLGA and PCL/PLGA/β-TCP membranes, whereas in osteogenic medium, ALP activity in ADSCs cultured on PCL/PLGA/β-TCP membranes was significantly higher than that on PCL/PLGA membranes ($p < 0.001$) (Fig. 3d). As shown in the results for the normal culture medium, β-TCP may not directly induce the osteogenic differentiation of ADSCs. However, the osteogenic differentiation of ADSCs was significantly promoted by β-TCP in the osteogenic medium in which osteogenic differentiation was induced. The increased gene expression and ALP activity on PCL/PLGA/β-TCP may result from the greater number of proliferating cells and the β-TCP, which affects the osteogenic differentiation of stem cells.[33]

### *Mineralization of ADSCs on the PCL/PLGA and PCL/PLGA/β-TCP membranes*

Calcium deposition of ADSCs, measured using a calcium assay kit, was significantly higher on PCL/PLGA/β-TCP membranes than on PCL/PLGA membranes at day 21, in both normal and osteogenic culture media (Fig. 4a). In osteogenic culture medium, calcium in ADSCs cultured on PCL/PLGA/β-TCP membranes was 2.75-fold of that in ADSCs on PCL/PLGA membranes (Fig. 4a). In addition, Alizarin Red S staining, which identifies calcium deposition in cultured cells or tissues, was used to visualize the mineralization of ADSCs cultured on the membranes. The ADSCs cultured on PCL/PLGA/β-TCP (Fig. 4d, e) showed greater mineralization than those on PCL/PLGA (Fig. 4b, c) at day 21, in both the normal and differentiation media. By contrast, β-TCP incorporated in the PCL/PLGA membrane was not stained by Alizarin Red S (Fig. 4f). This confirmed that the red-stained portion appearing in the membranes with ADSCs was completely attributable to calcium deposition with the ADSCs on the membranes. Furthermore, the degree of staining was quantified in a colorimetric analysis, revealing that the staining of ADSCs cultured on PCL/

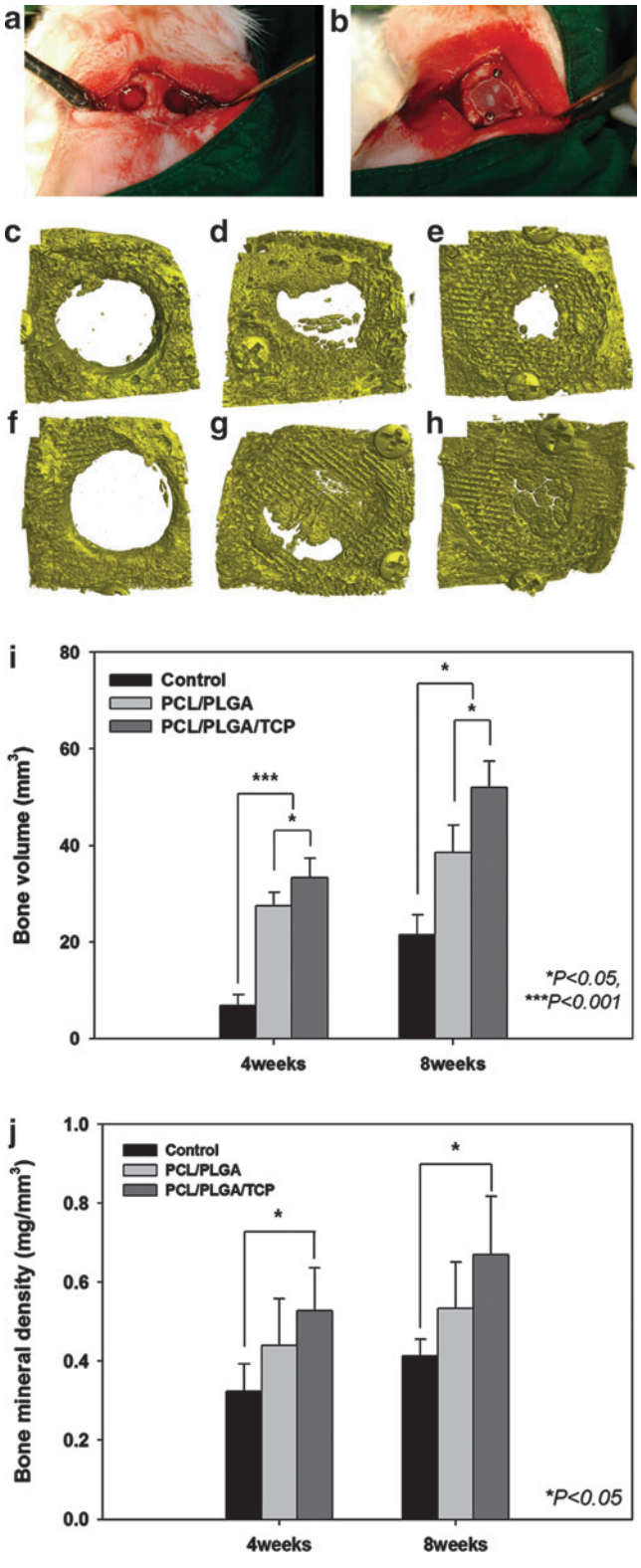


**FIG. 5.** *In vivo* bilateral full-thickness rabbit calvarial defects. **(a)** Two 8-mm-diameter defects were created. **(b)** The blended PCL/PLGA or PCL/PLGA/β-TCP membranes were placed randomly on the calvarial defects and fixed with titanium pins. μCT images were taken at 4 **(c, d, e)** and 8 **(f, g, h)** weeks after surgery. **(c, f)** control group, **(d, g)** PCL/PLGA group, **(e, h)** PCL/PLGA/β-TCP group. Numerical analysis of the *in vivo* experiments (the number of repeats = 6). **(i)** Bone volume in the defect ($mm^3$). **(j)** Bone mineral density ($mg/mm^3$) based on the μCT analysis. The bone volume was significantly higher in the PCL/PLGA and PCL/PLGA/β-TCP groups than in the control group, but only the PCL/PLGA/β-TCP group had a higher bone mineral density than the control group. μCT, microcomputed tomography. Color images available online at www.liebertpub.com/tea

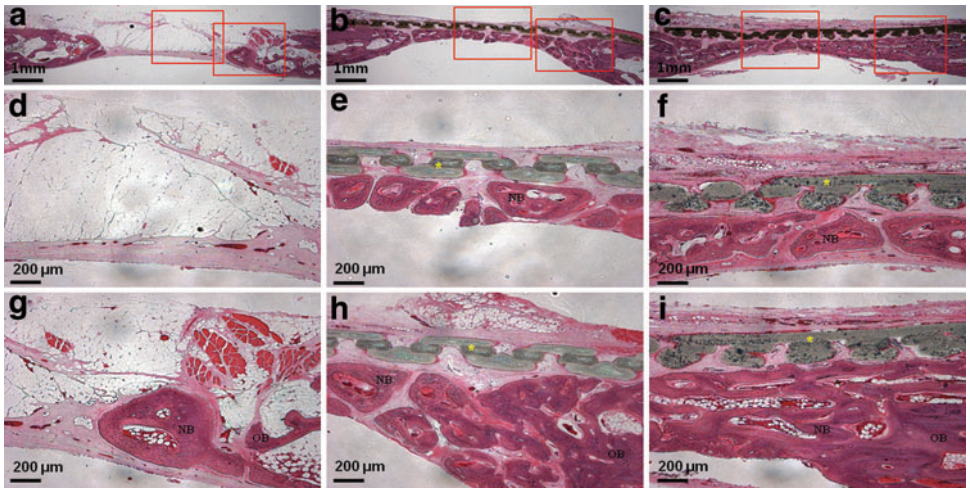


**FIG. 6.** Histological sections 4 weeks after surgery. **(a, d, g)** Uncovered control group. New bone formation is seen from the cut edge. **(b, e, h)** PCL/PLGA group. The membrane was not absorbed, and new bone formation is observed beneath the membrane. **(c, f, i)** PCL/PLGA/β-TCP group. The membrane was not absorbed, and there was more new bone than in the PCL/PLGA group. There was no inflammatory reaction around the membrane. Magnification, ×12.5 in **(a, b, c)** and ×40 in the others. Left and right rectangles in **(a, b, c)** indicate the observation zones of **(d, e, f)** and **(g, h, i)** respectively. Color images available online at www.liebertpub.com/tea

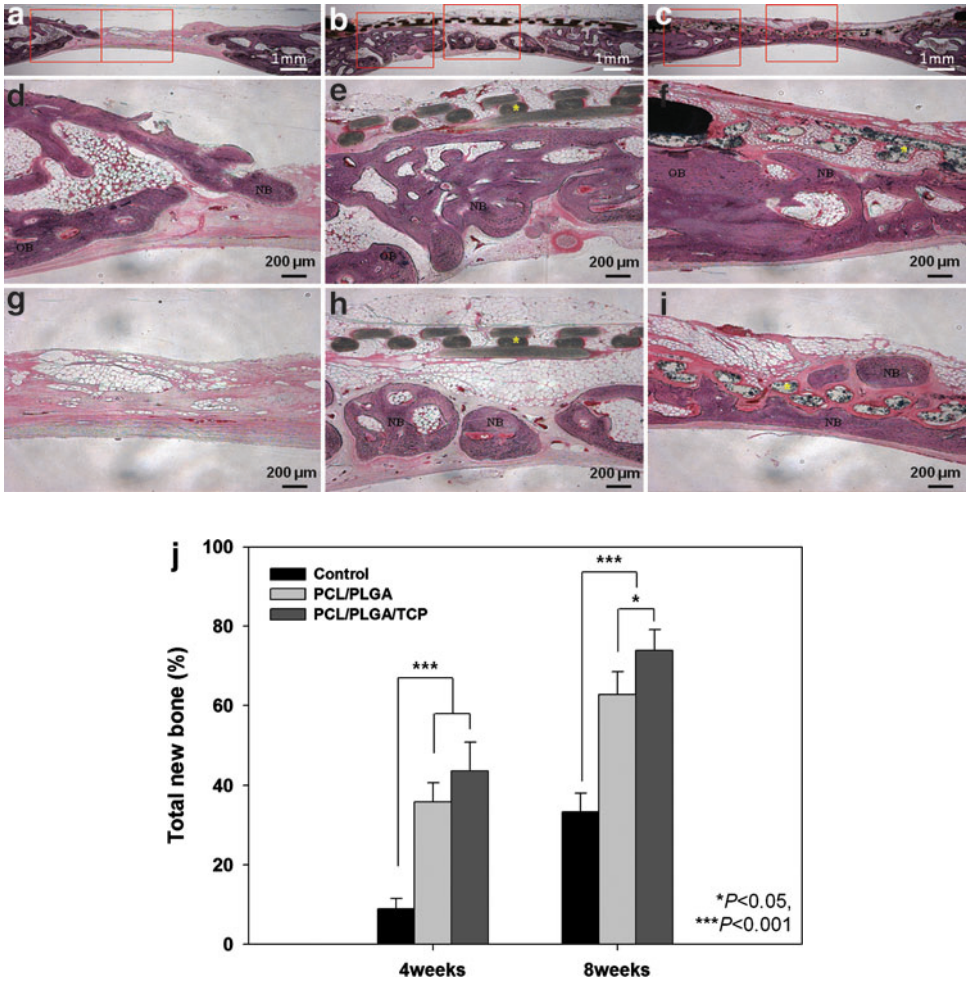


**FIG. 7.** Histological sections 8 weeks after surgery. **(a, d, g)** Uncovered control group. **(b, e, h)** PCL/PLGA group. The membrane was not absorbed, and new bone formation is observed beneath the membrane. **(c, f, i)** PCL/PLGA/β-TCP group. The membrane was absorbed partially, and new bone was formed continuously. It was difficult to distinguish between old and new bone. Magnification, ×12.5 in **(a, b, c)** and ×40 in the others. The histomorphometric analysis of **(j)** total new bone formation in the defect. Left and right rectangles in **(a, b, c)** indicate the observation zones of **(d, e, f)** and **(g, h, i)** respectively. Color images available online at www.liebertpub.com/tea

PLGA/β-TCP membranes was eight times the staining of ADSCs cultured on PCL/PLGA membranes in osteogenic culture medium (Fig. 4g). This suggests that the measurement of calcium using Alizarin Red solution in ADSCs on membranes was similar to the calcium deposition results shown in Figure 4a. Approximately 30% of the β-TCP loaded in polylactic acid fibers is reported to be degraded after 18 days in culture medium.[34] The calcium ions produced during β-TCP degradation, enhanced mineralization, which generally occurs in the last stage of osteogenic differentiation.[33–35] Thus, PCL/PLGA/β-TCP membranes promote osteogenic differentiation of ADSCs by increasing the number of proliferated cells and releasing calcium ions produced during the β-TCP degradation process.

### In vivo *new bone formation result of PCL/PLGA and PCL/PLGA/β-TCP membranes*

The μCT analysis results are presented in Figure 5c–j. The average values of the two measured variables were higher in the PCL/PLGA/β-TCP group than in the control group at both 4 and 8 weeks ($p<0.05$). Bone volumes in the control, PCL/PLGA, and PCL/PLGA/β-TCP groups 4 weeks after surgery were $7.74\pm3.03$, $26.06\pm4.20$, and $31.78\pm6.81\,mm^3$, respectively (Fig. 5i). There was a significant difference between each pair of groups ($p<0.05$). Bone mineral densities in the control, PCL/PLGA, and PCL/PLGA/β-TCP groups 4 weeks after surgery were $0.34\pm0.08$, $0.40\pm0.13$, and $0.51\pm0.11\,mg/mm^3$, respectively (Fig. 5j), and only the values in the control and PCL/PLGA/β-TCP groups ($p<0.05$) differed significantly. At 8 weeks after surgery, bone volumes in the control, PCL/PLGA, and PCL/PLGA/β-TCP groups were $22.83\pm4.80$, $40.31\pm6.70$, and $48.74\pm9.46\,mm^3$, respectively (Fig. 5i), with a significant difference between each pair of groups ($p<0.05$). Moreover, the majority of the 8-mm calvarial defects were closed by newly regenerated bone (Fig. 5h). Bone mineral densities in the control, PCL/PLGA, and PCL/PLGA/β-TCP groups 8 weeks after surgery were $0.46\pm0.11$, $0.50\pm0.13$, and $0.64\pm0.16\,mg/mm^3$, respectively (Fig. 5j). The values in the control and PCL/PLGA/β-TCP groups ($p<0.05$) were significantly different. Histological sectioning revealed active formation of an osteoid island identified by newly formed bone beneath the PCL/PLGA and PCL/PLGA/β-TCP membranes at both 4 (Fig. 6) and 8 weeks (Fig. 7). The PCL/PLGA and PCL/PLGA/β-TCP membranes had retained their shape without significant collapse at 4 weeks (Fig. 6b, c). In comparison, the collagen membrane had collapsed markedly, and a sunken area was observed at 4 weeks (Appendix Fig. A3a). This suggests that PCL/PLGA and PCL/PLGA/β-TCP membranes functioned as efficient GBR membranes *in vivo* with respect to mechanical properties. In addition, the soft tissue and membranes were tightly integrated (Fig. 6e, f), possibly owing to the porous and fully interconnected structure of the membrane.[36,37] This attribute may reduce traditional GBR issues regarding membrane separation and exposure. Importantly, osteoid islands had fused and healed completely in the PCL/PLGA/β-TCP group by 8 weeks, without the use of any bone substitute materials. Furthermore, obvious corticalization was observed at the center area of the defect (Fig. 7i). Infiltration of soft tissues into the area of new bone was greater with the collagen membrane than with the PCL/PLGA or PCL/PLGA/β-TCP membranes at 4 weeks. This infiltration, which should have been blocked by the membrane, can hinder the ingrowth of new bone. Indeed, discrete new bone formation with soft tissue located between the new bone islands was observed at 8 weeks in the collagen membrane group; this was distinct from the PCL/PLGA and PCL/PLGA/β-TCP groups, which showed continuous, integrated new bone formation. In addition, the PCL/PLGA/β-TCP membranes appeared more degraded than the PCL/PLGA membranes at 8 weeks (Fig. 7e, f), which may be related to the higher degradation rate of β-TCP. The released calcium ions might have affected early corticalization in the PCL/PLGA/TCP membranes.[38] Lymphocytes and multinucleated giant cells were at low concentrations in each group, and there were no inflammatory reactions around the PCL/PLGA and PCL/PLGA/β-TCP membranes, although PLGA is known to cause an immune response via acidic byproducts produced during degradation.[39] Histomorphometric analyses showed that the total percentages of new bone formation in the control, PCL/PLGA, and PCL/PLGA/β-TCP groups 4 weeks after surgery were $9.46\pm2.67$, $33.18\pm7.92$, and $41.43\pm8.43\%$, respectively (Fig. 7j). These values were significantly different ($p<0.05$). At 8 weeks after surgery, the total percentages of new bone formation in the control, PCL/PLGA, and PCL/PLGA/β-TCP groups were $31.85\pm5.61$, $61.33\pm6.20$, and $70.33\pm10.04\%$, respectively (Fig. 7j). These values were also significantly different ($p<0.05$).

## Conclusions

In the present study, we developed a bioabsorbable GBR membrane based on SFF technology. The PCL/PLGA and PCL/PLGA/β-TCP membranes promoted new bone formation *in vitro* and *in vivo*. Soft tissue integration was actively induced by the membranes, and no significant membrane collapse was observed. Thus, the SFF-based PCL/PLGA and PCL/PLGA/β-TCP membranes are promising as commercially relevant GBR membranes satisfying the essential requirements for alveolar bone regeneration.

## Acknowledgments

This work was supported by the National Research Foundation of Korea (NRF) grant funded by the Korea government (MEST) (No. 2011-0000412)) and Basic Science Research Program through the National Research Foundation of Korea (NRF) funded by the Ministry of Education, Science and Technology (2012005122).

## Disclosure Statement

No competing financial interests exist.

## References

1. Buser, D., Halbritter, S., Hart, C., Bornstein, M.M., Grutter, L., Chappuis, V., and Belser, U.C. Early implant placement with simultaneous guided bone regeneration following single-tooth extraction in the esthetic zone: 12-month results of a prospective study with 20 consecutive patients. J Periodontol **80,** 152, 2009.
2. Schwarz, F., Rothamel, D., Herten, M., Wustefeld, M., Sager, M., Ferrari, D., and Becker, J. Immunohistochemical

characterization of guided bone regeneration at a dehiscence-type defect using different barrier membranes: an experimental study in dogs. Clin Oral Implants Res **19,** 402, 2008.
3. Simion, M., Dahlin, C., Rocchietta, I., Stavropoulos, A., Sanchez, R., and Karring, T. Vertical ridge augmentation with guided bone regeneration in association with dental implants: an experimental study in dogs. Clin Oral Implants Res **18,** 86, 2007.
4. Urban, I.A., Jovanovic, S.A., and Lozada, J.L. Vertical ridge augmentation using guided bone regeneration (GBR) in three clinical scenarios prior to implant placement: a retrospective study of 35 patients 12 to 72 months after loading. Int J Oral Maxillofac Implants **24,** 502, 2009.
5. Lindfors, L.T., Tervonen, E.A., Sandor, G.K., and Ylikontiola, L.P. Guided bone regeneration using a titanium-reinforced ePTFE membrane and particulate autogenous bone: the effect of smoking and membrane exposure. Oral Surg Oral Med Oral Pathol Oral Radiol Endod **109,** 825, 2010.
6. Degidi, M., Scarano, A., and Piattelli, A. Regeneration of the alveolar crest using titanium micromesh with autologous bone and a resorbable membrane. J Oral Implantol **29,** 86, 2003.
7. Watzinger, F., Luksch, J., Millesi, W., Schopper, C., Neugebauer, J., Moser, D., and Ewers, R. Guided bone regeneration with titanium membranes: a clinical study. Br J Oral Maxillofac Surg **38,** 312, 2000.
8. Verardi, S., and Simion, M. Management of the exposure of e-PTFE membranes in guided bone regeneration. Pract Proced Aesthet Dent **19,** 111, 2007.
9. Chiapasco, M., and Zaniboni, M. Clinical outcomes of GBR procedures to correct peri-implant dehiscences and fenestrations: a systematic review. Clin Oral Implants Res **20 Suppl 4,** 113, 2009.
10. Jovanovic, S.A., Hunt, D.R., Bernard, G.W., Spiekermann, H., Wozney, J.M., and Wikesjo, U.M. Bone reconstruction following implantation of rhBMP-2 and guided bone regeneration in canine alveolar ridge defects. Clin Oral Implants Res **18,** 224, 2007.
11. von Arx, T., and Buser, D. Horizontal ridge augmentation using autogenous block grafts and the guided bone regeneration technique with collagen membranes: a clinical study with 42 patients. Clin Oral Implants Res **17,** 359, 2006.
12. Jung, R.E., Halg, G.A., Thoma, D.S., and Hammerle, C.H. A randomized, controlled clinical trial to evaluate a new membrane for guided bone regeneration around dental implants. Clin Oral Implants Res **20,** 162, 2009.
13. Fujihara, K., Kotaki, M., and Ramakrishna, S. Guided bone regeneration membrane made of polycaprolactone/calcium carbonate composite nano-fibers. Biomaterials **26,** 4139, 2005.
14. Jung, R.E., Lecloux, G., Rompen, E., Ramel, C.F., Buser, D., and Hammerle, C.H. A feasibility study evaluating an *in situ* formed synthetic biodegradable membrane for guided bone regeneration in dogs. Clin Oral Implants Res **20,** 151, 2009.
15. Schwarz, F., Herten, M., Ferrari, D., Wieland, M., Schmitz, L., Engelhardt, E., and Becker, J. Guided bone regeneration at dehiscence-type defects using biphasic hydroxyapatite+beta tricalcium phosphate (Bone Ceramic) or a collagen-coated natural bone mineral (BioOss Collagen): an immunohistochemical study in dogs. Int J Oral Maxillofac Surg **36,** 1198, 2007.
16. Kinoshita, Y., Matsuo, M., Todoki, K., Ozono, S., Fukuoka, S., Tsuzuki, H., Nakamura, M., Tomihata, K., Shimamoto, T., and Ikada, Y. Alveolar bone regeneration using absorbable poly(L-lactide-co-epsilon-caprolactone)/beta-tricalcium phosphate membrane and gelatin sponge incorporating basic fibroblast growth factor. Int J Oral Maxillofac Surg **37,** 275, 2008.
17. Oh, T.J., Meraw, S.J., Lee, E.J., Giannobile, W.V., and Wang, H.L. Comparative analysis of collagen membranes for the treatment of implant dehiscence defects. Clin Oral Implants Res **14,** 80, 2003.
18. Park, J.K., Yeom, J., Oh, E.J., Reddy, M., Kim, J.Y., Cho, D.W., Lim, H.P., Kim, N.S., Park, S.W., Shin, H.I., Yang, D.J., Park, K.B., and Hahn, S.K. Guided bone regeneration by poly(lactic-co-glycolic acid) grafted hyaluronic acid bi-layer films for periodontal barrier applications. Acta Biomater **5,** 3394, 2009.
19. Hutmacher, D.W., Sittinger, M., and Risbud, M.V. Scaffold-based tissue engineering: rationale for computer-aided design and solid free-form fabrication systems. Trends Biotechnol **22,** 354, 2004.
20. Jung, J.W., Kang, H.W., Kang, T.Y., Park, J.H., Park, J., and Cho, D.W. Projection Image-generation algorithm for fabrication of a complex structure using projection-based microstereolithography. Int J Precis Eng Manufact **13,** 445, 2012.
21. Kim, J.Y., Jin, G.Z., Park, I.S., Kim, J.N., Chun, S.Y., Park, E.K., Kim, S.Y., Yoo, J., Kim, S.H., Rhie, J.W., and Cho, D.W. Evaluation of solid free-form fabrication-based scaffolds seeded with osteoblasts and human umbilical vein endothelial cells for use *in vivo* osteogenesis. Tissue Eng Part A **16,** 2229, 2010.
22. Shim, J.H., Kim, J.Y., Park, M., Park, J., and Cho, D.W. Development of a hybrid scaffold with synthetic biomaterials and hydrogel using solid freeform fabrication technology. Biofabrication **3,** 034102, 2011.
23. Zhu, Y., Liu, T., Song, K., Fan, X., Ma, X., and Cui, Z. Adipose-derived stem cell: a better stem cell than BMSC. Cell Biochem Funct **26,** 664, 2008.
24. Diego, R.B., Estelles, J.M., Sanz, J.A., Garcia-Aznar, J.M., and Sanchez, M.S. Polymer scaffolds with interconnected spherical pores and controlled architecture for tissue engineering: fabrication, mechanical properties, and finite element modeling. J Biomed Mater Res B Appl Biomater **81,** 448, 2007.
25. Jeon, O., Rhie, J.W., Kwon, I.K., Kim, J.H., Kim, B.S., and Lee, S.H. *In vivo* bone formation following transplantation of human adipose-derived stromal cells that are not differentiated osteogenically. Tissue Eng Part A **14,** 1285, 2008.
26. Arpornmaeklong, P., Brown, S.E., Wang, Z., and Krebsbach, P.H. Phenotypic characterization, osteoblastic differentiation, and bone regeneration capacity of human embryonic stem cell-derived mesenchymal stem cells. Stem Cells Dev **18,** 955, 2009.
27. Tsai, S.W., Liou, H.M., Lin, C.J., Kuo, K.L., Hung, Y.S., Weng, R.C., and Hsu, F.Y. MG63 osteoblast-like cells exhibit different behavior when grown on electrospun collagen matrix versus electrospun gelatin matrix. PLoS One **7,** e31200, 2012.
28. Kim, J.Y., Park, J.K., Hahn, S.K., Kwon, T.H., and Cho, D.-W. Development of the flow behavior model for 3D scaffold fabrication in the polymer deposition process by a heating method. J Micromech Microeng **19,** 105003, 2009.
29. Sun, H., Mei, L., Song, C., Cui, X., and Wang, P. The *in vivo* degradation, absorption and excretion of PCL-based implant. Biomaterials **27,** 1735, 2006.

30. Sung, H.J., Meredith, C., Johnson, C., and Galis, Z.S. The effect of scaffold degradation rate on three-dimensional cell growth and angiogenesis. Biomaterials **25,** 5735, 2004.
31. Lam, C.X.F., Teoh, S.H., and Hutmacher, D.W. Comparison of the degradation of polycaprolactone and polycaprolactone–(β-tricalcium phosphate) scaffolds in alkaline medium. Polym Int **56,** 718, 2007.
32. Deligianni, D.D., Katsala, N.D., Koutsoukos, P.G., and Missirlis, Y.F. Effect of surface roughness of hydroxyapatite on human bone marrow cell adhesion, proliferation, differentiation and detachment strength. Biomaterials **22,** 87, 2001.
33. Takahashi, Y., Yamamoto, M., and Tabata, Y. Osteogenic differentiation of mesenchymal stem cells in biodegradable sponges composed of gelatin and beta-tricalcium phosphate. Biomaterials **26,** 3587, 2005.
34. McCullen, S.D., Zhu, Y., Bernacki, S.H., Narayan, R.J., Pourdeyhimi, B., Gorga, R.E., and Loboa, E.G. Electrospun composite poly(L-lactic acid)/tricalcium phosphate scaffolds induce proliferation and osteogenic differentiation of human adipose-derived stem cells. Biomed Mater **4,** 035002, 2009.
35. Liu, Q., Cen, L., Yin, S., Chen, L., Liu, G., Chang, J., and Cui, L. A comparative study of proliferation and osteogenic differentiation of adipose-derived stem cells on akermanite and beta-TCP ceramics. Biomaterials **29,** 4792, 2008.
36. Feng, B., Jinkang, Z., Zhen, W., Jianxi, L., Jiang, C., Jian, L., Guolin, M., and Xin, D. The effect of pore size on tissue ingrowth and neovascularization in porous bioceramics of controlled architecture *in vivo*. Biomed Mater **6,** 015007, 2011.
37. Ryan, G., Pandit, A., and Apatsidis, D.P. Fabrication methods of porous metals for use in orthopaedic applications. Biomaterials **27,** 2651, 2006.
38. Arinzeh, T.L., Tran, T., Mcalar, J., and Daculsi, G. A comparative study of biphasic calcium phosphate ceremics for human mesenchymal stem-cell-induced bone formation. Biomaterials **26,** 3631, 2005.
39. Lickorish, D., Guan, L., and Davies, J.E. A three-phase, fully resorbable, polyester/calcium phosphate scaffold for bone tissue engineering: evolution of scaffold design. Biomaterials **28,** 1495, 2007.

Address correspondence to:
*Dong-Woo Cho, PhD*
*Division of Integrative Biosciences and Biotechnology*
*Department of Mechanical Engineering*
*POSTECH*
*San 31 Hyoja-dong, Nam-gu*
*Pohang*
*Gyungbuk 790-784*
*Korea*

*E-mail:* dwcho@postech.ac.kr

*Received: December 22, 2011*
*Accepted: August 13, 2012*
*Online Publication Date: October 4, 2012*

(*Appendix follows* →)

# Appendix

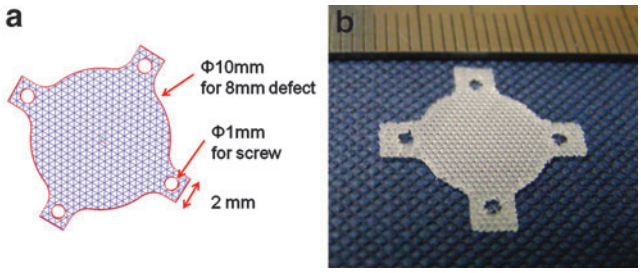


**APPENDIX FIG. A1.** Design of membrane for *in vivo* experiment: **(a)** designed membrane by computer-aided design/computer-aided manufacturing process and **(b)** fabricated membrane. Four wing parts with circular holes (1 mm diameter) were constructed every 90° in the circular membranes to fix the membrane with titanium screws. This particular design is possible only with solid freeform fabrication technology. Color images available online at www.liebertpub.com/tea

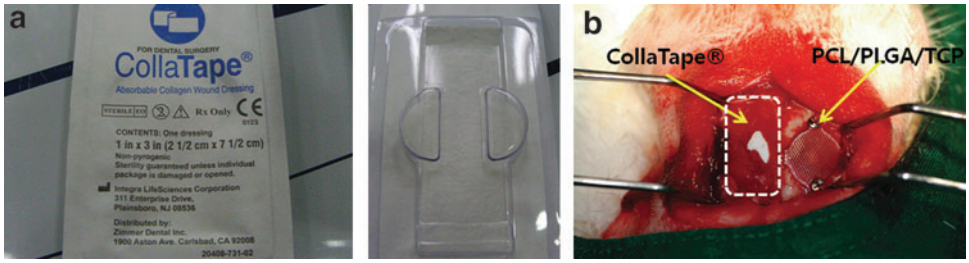


**APPENDIX FIG. A2.** Comparative *in vivo* experiments: **(a)** Commercially available collagen membrane (CollaTape®), and **(b)** implantation of collagen and PCL/PLGA/β-TCP membranes on the rabbit calvarial defect. The collagen membrane results were not reported in the main manuscript due to the insufficient number of samples. However, the obvious collapse of the collagen membrane resulted in less bone regeneration compared with the PCL/PLGA and PCL/PLGA/β-TCP membranes. PCL, polycaprolactone; PLGA, poly(lactic-co-glycolic acid); β-TCP, beta-tricalcium phosphate. Color images available online at www.liebertpub.com/tea

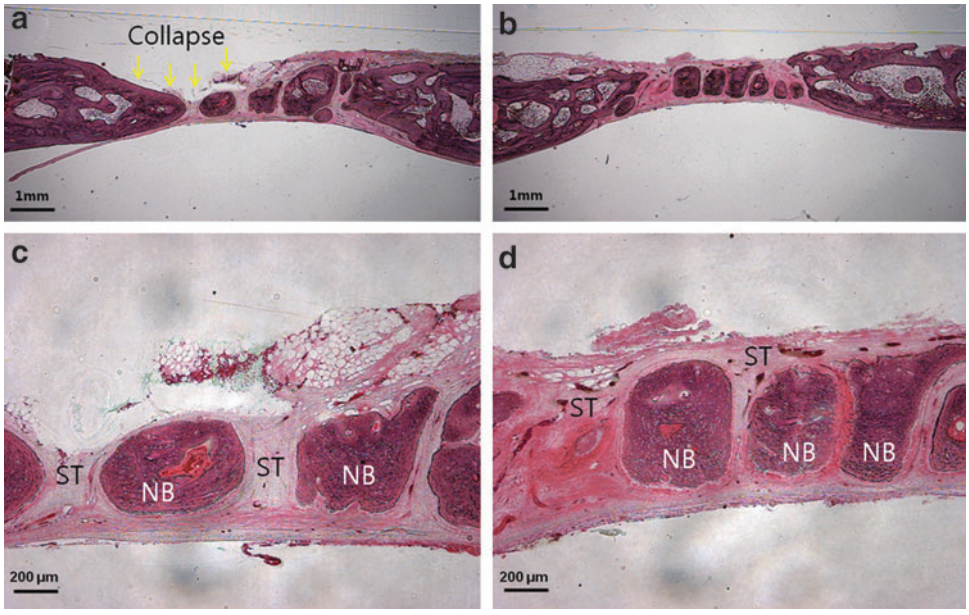


**APPENDIX FIG. A3.** Histologic section of collagen membrane groups at 4 **(a, c)** and 8 **(b, d)** weeks after implantation: **(a)** Membrane was collapsed and absorbed at 4 weeks. **(c, d)** Abundant infiltration of ST between the NB was observed, and discrete NB was formed. (Magnifications were ×12.5 in Division of Integrative Biosciences and Biotechnology, and ×40 in others.) ST, soft tissue; NB, new bone. Color images available online at www.liebertpub.com/tea